WHITE PAPER July 2026

EPR Pulsed Dipolar Spectroscopy for Structural Biology

A complementary approach to Cryo-EM, AlphaFold, and other methods, enabled by the FATHOM® automated EPR spectrometer

High Q Technologies Inc.

Abstract

Proteins are molecular machines, and much of what they do depends on movement. They bend, flex, and switch between shapes, and the parts that move the most are often the parts that matter most for health, for disease, and for the design of new medicines. Yet most methods for determining protein structure capture a single frozen snapshot or an average over many molecules, so the movement itself, and the existence of more than one shape at once, can be missed.

Electron paramagnetic resonance (EPR) pulsed dipolar spectroscopy (PDS) takes a different approach. By attaching two tiny magnetic tags to a molecule, it measures the distance between them and, just as importantly, how much that distance varies. This provides a direct readout of flexibility and of the different shapes a molecule adopts. EPR does not replace methods such as Cryo-EM or the structure-prediction tool AlphaFold; it works alongside them, supplying the information about motion and multiple states that those methods do not easily capture on their own.

For decades, EPR has been confined to specialist laboratories because it required liquid cryogens, custom hardware, and considerable expertise. The FATHOM automated EPR spectrometer is designed to remove those barriers. It needs no liquid cryogens, runs measurements automatically, and is intended to be used by scientists and technicians who are not EPR specialists, so that this uniquely informative technique can become a routine part of the modern structural biology and drug-discovery laboratory. This white paper explains what EPR PDS measures, how it complements the other tools of structural biology, and how FATHOM makes them practical.

1. Introduction

Structural biology has entered an era of remarkable capability. The resolution revolution in cryo-electron microscopy has made near-atomic structures of large complexes almost routine, and AlphaFold and related tools now predict how entire proteomes fold, based only on the amino acid sequences. The picture these advances provide is, however, largely a static one. Proteins function through motion: they cycle between conformations, flex at hinges and loops, assemble and disassemble, and in many cases contain regions that are intrinsically disordered and never adopt a single fixed structure.

These dynamic and disordered features are precisely what static, averaged, or predicted structures resolve least well, and they are increasingly the features that determine biological mechanism and therapeutic opportunity. Intrinsically disordered regions (IDRs), in particular, have moved from the periphery of structural biology toward the center of drug discovery, where they present both new targets and new challenges (Lazar et al. 2025). The pressing gap in the structural biologist's toolkit is therefore not one of resolution but of dynamics and heterogeneity. The most pressing need is to measure conformational ensembles, flexibility, and coexisting states directly.

EPR PDS addresses this need: by measuring the distance distribution between pairs of spin labels, it reports directly on conformational ensembles, on the flexibility of a region, and on the populations of coexisting states, over a range of roughly 1.5 to 8 nm and with no ceiling on molecular size. Measurements can be made in solution, in lipid bilayers and nanodiscs, and even inside cells, in conditions close to the native environment. The information refines that provided by other methods, which is what makes EPR a natural complement to them, rather than a competitor.

If the value of this information is well established, why is EPR not already standard? The answer has been instrumentation rather than utility. Conventional pulsed EPR has demanded liquid cryogens, specialized hardware, and expert operation, confining it to a small number of specialized laboratories. Recent advances in superconducting resonator EPR systems, embodied in the FATHOM platform, change this calculus by delivering the necessary sensitivity on small, dilute samples while automating the measurement (Gamble Jarvi et al. 2026).

The remainder of this paper develops these points in turn. Section 2 is a primer on what EPR and pulsed dipolar spectroscopy actually measure. Section 3 sets EPR within the structural biology toolkit and details its complementarity with each major method. Section 4 presents application case studies drawn from the published literature. Section 5 describes the FATHOM instrument and how it makes routine EPR practical. Section 6 offers a brief outlook.

2. What EPR and Pulsed Dipolar Spectroscopy Measure

2.1 EPR in brief

Electron paramagnetic resonance (EPR), also called electron spin resonance (ESR), is the electron-spin counterpart of nuclear magnetic resonance (NMR). Where NMR detects nuclear spins, EPR detects unpaired electron spins, which are far more sensitive to their immediate surroundings. A sample is placed in a magnetic field and irradiated with microwaves, and the way the unpaired electrons respond reports on their local environment, and their distance from other unpaired electrons. Because the readout depends on the spins rather than on the mass or crystallinity of the molecule, EPR is conceptually parallel to NMR but without the molecular-size ceiling that limits solution NMR, and with much higher sensitivity to conformation (Galazzo, Teucher, and Bordignon 2022).

2.2 Spin labels as reporters

The standard sample preparation approach is called site-directed spin labeling (SDSL): one or more stable radical tags are attached at chosen positions, most commonly nitroxide labels coupled to engineered cysteine residues. Placing two labels at defined sites turns a structural question into a distance measurement. A growing palette of orthogonal labels, including gadolinium, copper, and trityl centers, extends the method to multi-distance experiments and to more demanding conditions (Galazzo, Teucher, and Bordignon 2022). In some systems no engineered label is required at all: native paramagnetic centers such as protein-bound Cu(II) can serve directly as the reporters, allowing label-free distance measurements in metalloproteins (Merz et al. 2014).

2.3 From spins to distances: pulsed dipolar spectroscopy

The distance between two electron spins is encoded in their magnetic dipolar coupling, which scales with the inverse cube of the separation. Pulsed dipolar spectroscopy (PDS) isolates this coupling using tailored microwave pulse sequences. The most widely used implementation is double electron-electron resonance (DEER, also called PELDOR), with related sequences such as RIDME and double-quantum coherence (DQC) suited to particular label types and distance regimes (Galazzo, Teucher, and Bordignon 2022; Roy et al. 2025). The experiment produces a time-domain signal whose modulation frequency reflects the interspin distance and whose damping reflects the spread of distances. Converting this signal yields a distance distribution, P(r): an Angström-level quantitative picture of how far apart the labels are and how much that separation varies across the sample.

2.4 Reading a distance distribution

The distance distribution is the central output and is intuitive to interpret. The position of a peak gives the most probable interspin distance. The width of a peak reports on flexibility: a rigid, well-defined structure produces a narrow peak, whereas a flexible or dynamic region produces a broad one. When a molecular ensemble exists in more than one conformation, the distribution becomes multimodal, with each peak corresponding to a coexisting state and the relative peak areas reflecting their populations. This ability to resolve and quantify coexisting states, rather than reporting only an average, is what makes PDS well suited to dynamics and disorder (Figure 2).

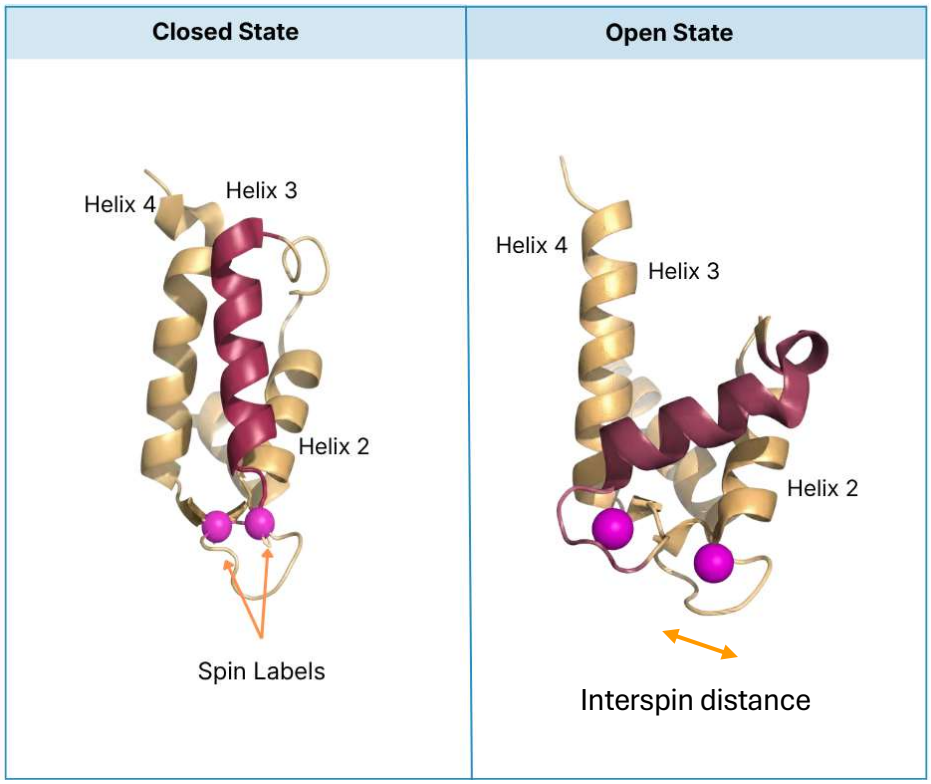

Figure 1. Site-directed spin labeling concept. A ribbon model of a protein, here a multi-helix motif, bearing two nitroxide spin labels attached at engineered cysteine sites, with the two labels marked and the through-space interspin separation indicated. The figure illustrates that pulsed dipolar spectroscopy measures the distance between the two labels. *Adapted from Narunsky et al. (2015), licensed under CC BY 4.0.*

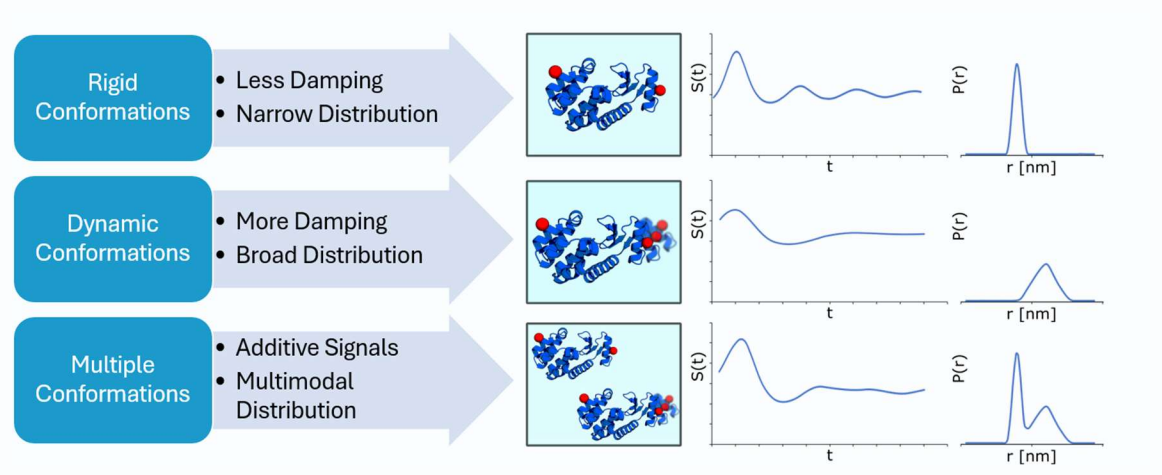

Figure 2. From the dipolar time-domain signal to a distance distribution P(r), shown for three conformational regimes. Each row pairs a representative time-domain DEER trace (signal S(t) versus time t) with the corresponding distance distribution (probability P(r) versus interspin distance r in nm). Top row, rigid single conformation: a slowly damped, clearly oscillatory trace yielding a narrow unimodal peak. Middle row, dynamic or flexible state: a rapidly damped trace yielding a single broad peak. Bottom row, multiple coexisting conformations: a composite trace yielding a multimodal distribution. The figure conveys that peak position encodes distance, peak width encodes flexibility, and multiple peaks reveal coexisting states, across a working range of roughly 1.5 to 8 nm. *Middle images adapted from PDB entry 3LZM (Matsumura et al. 1989).*

2.5 Working range, environment, and sensitivity

PDS typically measures distances over a range of roughly 1.5 to 8 nm, the length scale that spans most intramolecular interactions. Critically, the measurement does not depend on molecular weight, so it applies equally to small proteins and to megadalton assemblies. Measurements can be made not only in buffer but in lipid bilayers, nanodiscs, and even whole cells, providing information in environments close to the native one (Galazzo et al. 2020). Samples are typically flash-frozen and measured at cryogenic temperature to extend the spin coherence that the experiment relies on. Historically this combination of spin labeling, cryogenics, and specialized pulse hardware confined PDS to expert laboratories. Recent instrument advances made by High Q Technologies using superconducting resonators have brought the required sensitivity to small, dilute samples, below 10 micromolar, in volumes of a few microliters, and have added the automation needed for routine use (Gamble Jarvi et al. 2026), a point we return to in Section 5.

3. EPR in the Structural Biology Toolkit

3.1 The gap EPR fills

Modern structural biology resolves rigid, well-ordered structures with extraordinary success. The persistent gap lies in flexibility and disorder: loops, hinges, intrinsically disordered regions, and the coexisting conformational states through which many proteins actually function. These are increasingly the features that matter for biological mechanism and for drug discovery (Lazar et al. 2025). EPR-based PDS addresses this gap directly, because it measures distance distributions rather than a single static structure. Just as importantly, it does so in a way that complements other methods (Figure 3).

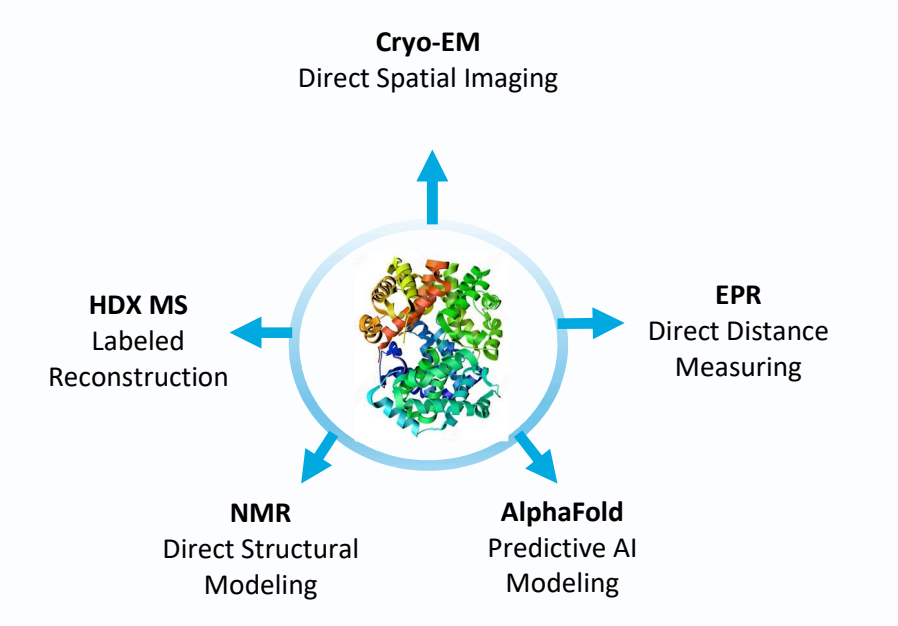

Figure 3. EPR positioned among complementary structural biology methods. A central macromolecule is surrounded by the principal techniques, each annotated by the kind of information it provides: Cryo-EM (direct spatial imaging), EPR (direct distance distribution), AlphaFold (predictive modeling), NMR (direct structural modeling), and HDX-MS (labeling and reconstruction). The arrangement conveys that EPR contributes orthogonal distance and dynamics information that complements other methods.

3.2 Cryo-EM

Cryo-EM resolves the global architecture of large complexes at near-atomic resolution, but flexible, disordered, or multi-conformational regions tend to get averaged out, lowering the confidence in those areas. EPR refines Cryo-EM structures by contributing direct distance information for exactly those regions where density is missing, exposing minor states that particle classification cannot isolate, and testing whether a modeled state is the dominant one. A map may show a closed state, for instance, while EPR distances reveal a predominantly open distribution, indicating a grid-stabilized rather than dominant conformation. The blurring that Cryo-EM treats as a limitation becomes, for EPR, the measurable quantity (Frank et al. 2016; Stock et al. 2018).

3.3 AlphaFold and AF-Multimer

AlphaFold predicts folds from sequences with remarkable accuracy, but it predicts disorder without predicting dynamics, and returns essentially a single model with limited ensemble insight (del Alamo et al.

2022). Regions of low confidence (low pLDDT) are frequently the flexible and disordered regions of greatest functional interest. EPR distance distributions validate and refine these low-confidence regions and can be integrated algorithmically: approaches such as DEERFold guide AlphaFold2 with experimental DEER restraints to generate conformational ensembles rather than single structures (Wu et al. 2025; del Alamo et al. 2022).

3.4 HDX-MS

Hydrogen-deuterium exchange mass spectrometry reports local backbone flexibility and solvent protection across very large complexes, with no size limit. It is, however, ensemble-averaged and cannot resolve discrete coexisting states, and topological information is lost before the mass readout (Konermann et al. 2011). EPR complements HDX-MS by converting regions flagged as dynamic into specific, quantified distances and by resolving the distinct states that HDX-MS data tends to average together.

3.5 NMR

Solution NMR provides atomic-resolution information on local environment and residue-specific dynamics, and it resolves multiple states through chemical shift and relaxation measurements. Its principal constraints are molecular size, with solution working best below roughly 50 to 70 kDa, and short range distance measurements via NOESY (0.5 nm or less; Honegger et al. 2021). Paramagnetic NMR, through paramagnetic relaxation enhancement (PRE) or pseudo contact shifts (PCS), together with ^{19}F labeling, extends this range to roughly 1 to 3 nm, often relying on the same nitroxide or metal labels used in PDS (Clore and Iwahara 2009). EPR extends distance measurements to roughly 8 nm and can be applied to systems regardless of molecular size.

3.6 X-ray crystallography

X-ray crystallography delivers atomic-resolution models of well-ordered regions but reports a single dominant conformation within a crystalline, non-native packing environment, and flexible regions rarely crystallize (Woldeyes et al. 2014). EPR supplies the missing dynamic and disordered information in solution, complementing the rigid-region detail that crystallography provides.

3.7 Fluorescence methods (FRET and smFRET)

Single-molecule FRET excels at watching transitions between states in real time, including in live cells, but provides limited structural detail and depends on fluorescent labeling and photophysics. EPR and FRET are conceptually allied, both being distance methods. EPR contributes a different and partly overlapping distance range, quantitative distance distributions, and applicability to systems where fluorophore behavior is limiting.

3.8 Molecular dynamics simulation

MD simulations generate full atomistic trajectories and are unmatched for mechanistic detail, but they require a starting structural model and accurate force fields, and their reliability is bounded by sampling. EPR distance distributions provide experimental restraints and validation for simulated ensembles, anchoring computation to measurement.

3.9 Summary comparison

The table below summarizes how the major methods compare across the dimensions that matter most for studying flexible and disordered systems. The recurring pattern is that EPR is rarely the only tool a laboratory needs, but it consistently supplies the dynamic, multi-state, and environmental information that the others do not measure directly.

Method	Size range	Dynamics & IDRs	Coexisting states	Native environment	Sample needs
EPR (DEER/PELDOR)	Any size; labels set the limits, not mass	Excellent for motions, distances, IDRs, flexible loops	Resolved and quantified via distance distributions	Lipids, nanodiscs, whole cells	Spin labeling or native paramagnetic centers
Cryo-EM	Best >100 kDa, up to megadalton	Limited for IDRs; density disappears	Major states if sufficiently populated	Frozen-hydrated; near-native but static	High purity, monodisperse; vitrification
AlphaFold / AF-Multimer	Any size (computational)	Predicts disorder but not dynamics	Single model; limited ensemble insight	In silico only	Sequence only; no experiment
HDX-MS	Any size; strong for large complexes	Strong for local flexibility, IDRs, protection	Ensemble-averaged; cannot resolve states	Solution; topology lost before readout	Proteolysis, LC-MS workflow
Fluorescence (FRET, smFRET)	Small to very large	Excellent for real-time dynamics	Tracks transitions; limited structural detail	In vitro or live cells	Fluorescent labeling; photophysics limits
Molecular dynamics (MD)	Any size (compute-limited)	Excellent for atomistic motions, IDRs, folding	Full trajectories; bounded by sampling	In silico; can mimic membranes, crowding	Needs a starting model and force fields
X-ray crystallography	Small to moderately large	Poor for dynamics; IDRs rarely crystallize	Single dominant conformation	Crystalline; non-native packing	Crystals; often excludes flexible regions
NMR spectroscopy	Best <50 to 70 kDa (solution)	Excellent for dynamics, IDRs, exchange	Multiple states via shifts and relaxation	Solution or solid-state; near-native	Isotopic labeling; conc. and stability limits

Table 1. Comparison of major structural biology methods across molecular size range, sensitivity to dynamics and intrinsically disordered regions, ability to resolve coexisting conformational states, environmental realism, and sample requirements. The EPR row is highlighted. Adapted and condensed from the FATHOM educational materials; method descriptions reflect general capabilities rather than any single study.

3.10 Integrative workflows

The greatest value of EPR is realized when its restraints are combined with the methods above. Distance distributions can refine low-density Cryo-EM regions, guide and validate AlphaFold ensembles through frameworks such as DEERFold, restrain MD trajectories, and support hybrid modeling pipelines (Wu et al. 2025; del Alamo et al. 2022; Frank et al. 2016). The result is not a replacement for any existing technique but an additional, orthogonal source of the dynamic and disorder information that the others cannot measure directly.

4. Application Case Studies

The following case studies illustrate how EPR and pulsed dipolar spectroscopy have been applied across the structural biology landscape. They are drawn from the peer-reviewed literature and grouped by the kind of problem EPR helps solve. In each, the theme of Sections 2 and 3 recurs: EPR supplies dynamic, multi-state, and distance information that complements the other methods rather than duplicating them.

4.1 Mapping conformational cycles alongside Cryo-EM

Membrane transporters move through a cycle of conformations, and the transitions between states are exactly what static structures struggle to capture. Stock et al. (2018) determined two cryo-EM structures of the 157 kDa KdpFABC potassium-uptake complex, in distinct E1 and E2 states, and proposed a transport mechanism running through two inter-subunit half-channels. Site-directed spin labeling and DEER distance measurements then tested the states underlying the model, providing solution-state distances for the dynamic regions of the cycle and comparing the expected distances from the cryo-EM coordinates against the EPR-measured distributions (Figure 4).

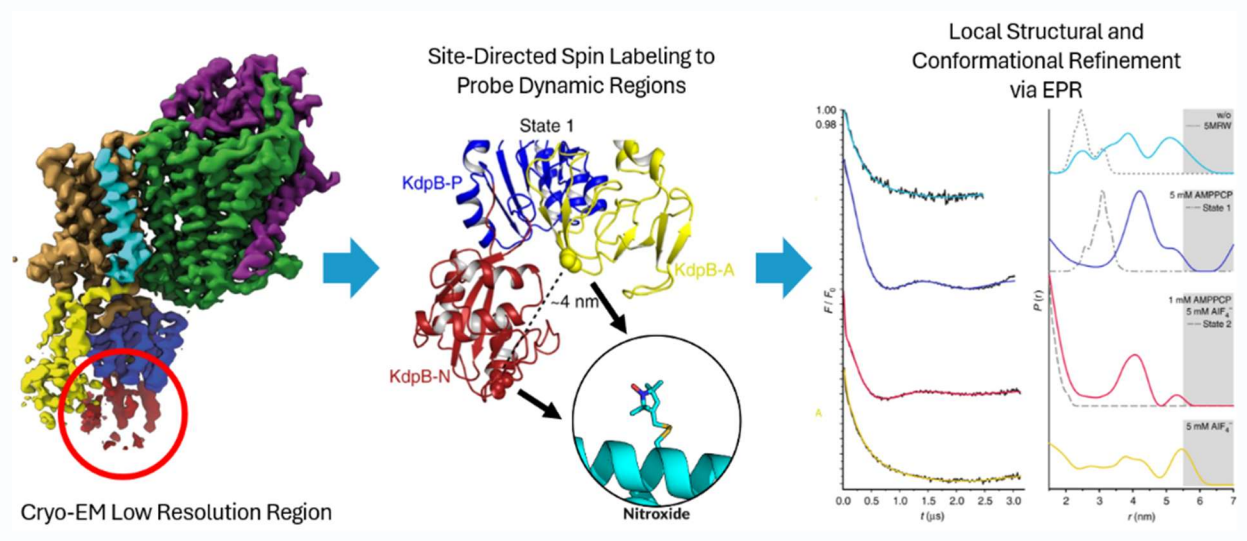

Figure 4. Cryo-EM and EPR working together on the KdpFABC transport cycle. A low-resolution flexible region of the cryo-EM map (left) is targeted by site-directed spin labeling to probe dynamic regions (center), and DEER time-domain traces are converted to distance distributions (right) that compare the distance expected from the cryo-EM coordinates with the EPR-measured distance. The comparison validates and refines the conformational states of the transport cycle. *Adapted from Stock et al. (2018), licensed under CC BY 4.0.*

Zhang et al. (2024) extended this integrative approach to a protease-containing ABC transporter, which couples ATP hydrolysis to the processing and export of cargo proteins. Combining single-particle cryo-EM, DEER spectroscopy in lipid nanodiscs, and computational analysis, they reconstructed the full conformational cycle and uncovered a competitive interplay between nucleotide and cargo-protein binding. The DEER measurements in bilayers revealed differences from the distances predicted by the cryo-EM structures, and the two data sources were combined to model the mechanistic pathway. In both systems, cryo-EM supplies the high-resolution endpoints while EPR supplies the solution-state distances and the transitions between them.

4.2 Building conformational ensembles with AlphaFold

AlphaFold returns a single high-confidence model, but transporters and other dynamic proteins exist as ensembles. del Alamo et al. (2022) integrated AlphaFold2 with DEER to investigate the conformational dynamics of GadC, a pH-dependent APC antiporter with the canonical LeuT fold that helps pathogenic bacteria survive acid stress by exchanging glutamate for GABA. By manipulating the prediction inputs to generate candidate conformations and testing them against experimental DEER distance distributions, they mapped inward- and outward-facing states that a single static prediction does not capture.

Wu et al. (2025) formalized this integration as DEERFold, a modified version of AlphaFold2 built on the OpenFold platform that incorporates DEER distance distributions directly into the network architecture. DEERFold switches the predicted conformations of membrane transporters using experimental distance distributions, and because the intrinsic accuracy of AlphaFold2 is high, only sparse sets of distributions are needed to steer the prediction toward the correct ensemble (Figure 5). Together, these studies turn AlphaFold from a single-structure predictor into an ensemble generator for precisely the low-confidence, flexible regions that are of greatest functional interest.

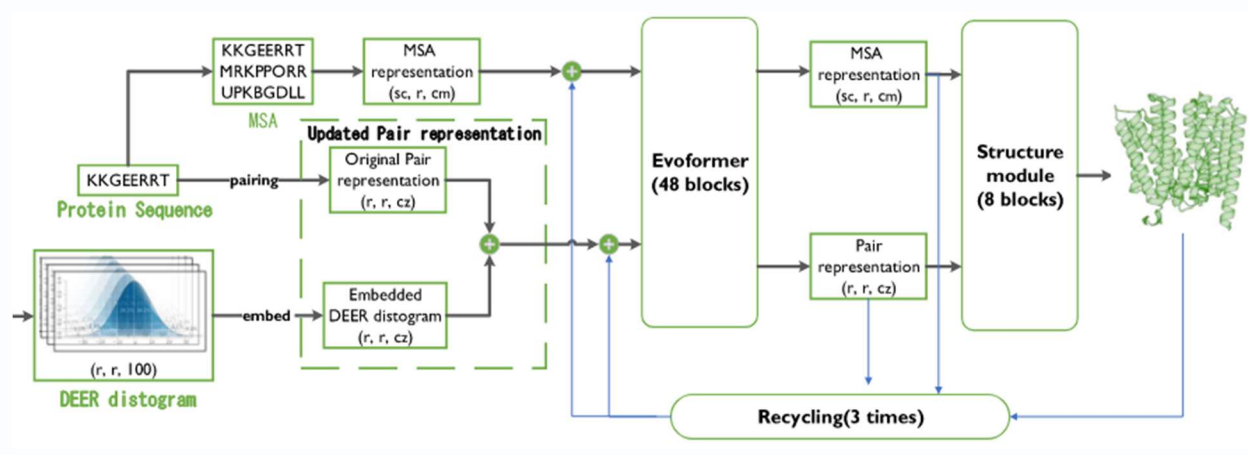

Figure 5. The DEERFold architecture. An experimental DEER distance distribution is embedded as a distogram and injected into the AlphaFold2 pipeline (MSA and pair representations, Evoformer blocks, and the structure module), so that EPR restraints guide the network toward experimentally consistent conformations rather than a single default prediction. *Adapted from Wu et al. (2025), used under license.*

4.3 Characterizing intrinsically disordered proteins

Intrinsically disordered proteins underlie essential cellular functions and drive the onset of neurodegenerative disease through mutation-induced structural changes, yet their conformational heterogeneity often evades crystallography and cryo-EM and is not captured by single-structure prediction. Roy et al. (2025) used double-quantum coherence (DQC) ESR, a PDS method, to detect mutation-induced conformational changes in an intrinsically disordered protein, comparing EPR-derived distance distributions on a tau fragment against AlphaFold predictions and cryo-EM data. The distance distributions revealed a broader conformational landscape than the other methods resolved, and quantified how a disease-linked mutation shifts that landscape (Figure 6). For the disordered regions that motivate this paper, EPR provides direct, quantitative ensemble information that is otherwise unavailable.

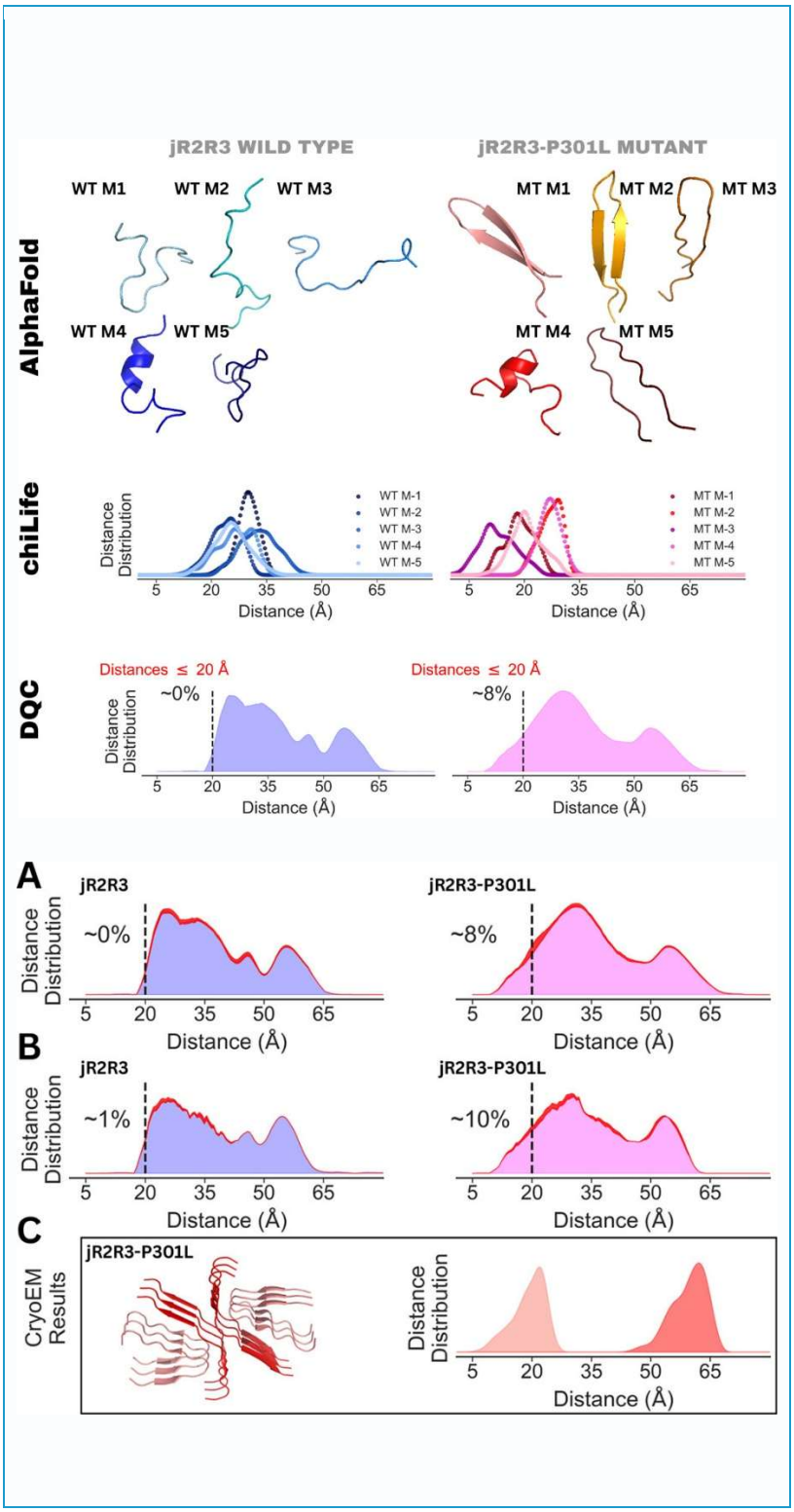

Figure 6. Probing an intrinsically disordered protein. For a tau fragment in wild-type and disease-mutant forms, AlphaFold models and cryo-EM data are compared with DQC ESR distance distributions. Where AlphaFold returns single representative structures and cryo-EM cannot resolve the disordered ensemble, the EPR distance distributions expose a broad conformational landscape and the population shift induced by mutation. *Adapted from Roy et al. (2025), reproduced here with permission from the authors.*

4.4 Detecting disease-linked conformational states

Some proteins carry native paramagnetic centers, allowing EPR to read out conformation with no engineered label at all. Merz et al. (2014) demonstrated label-free PDS on Cu-Zn superoxide dismutase (SOD1), a homodimer with one endogenous Cu(II) per monomer, using DEER to measure the dipolar coupling between the inherent copper ions. Differences in the resulting distance distributions corresponded to disease-associated mutations linked to amyotrophic lateral sclerosis (ALS), distinguishing wild-type from mutant conformations directly (Figure 7). Where a target carries native metal centers, EPR offers a label-free route to connecting conformational change with pathology.

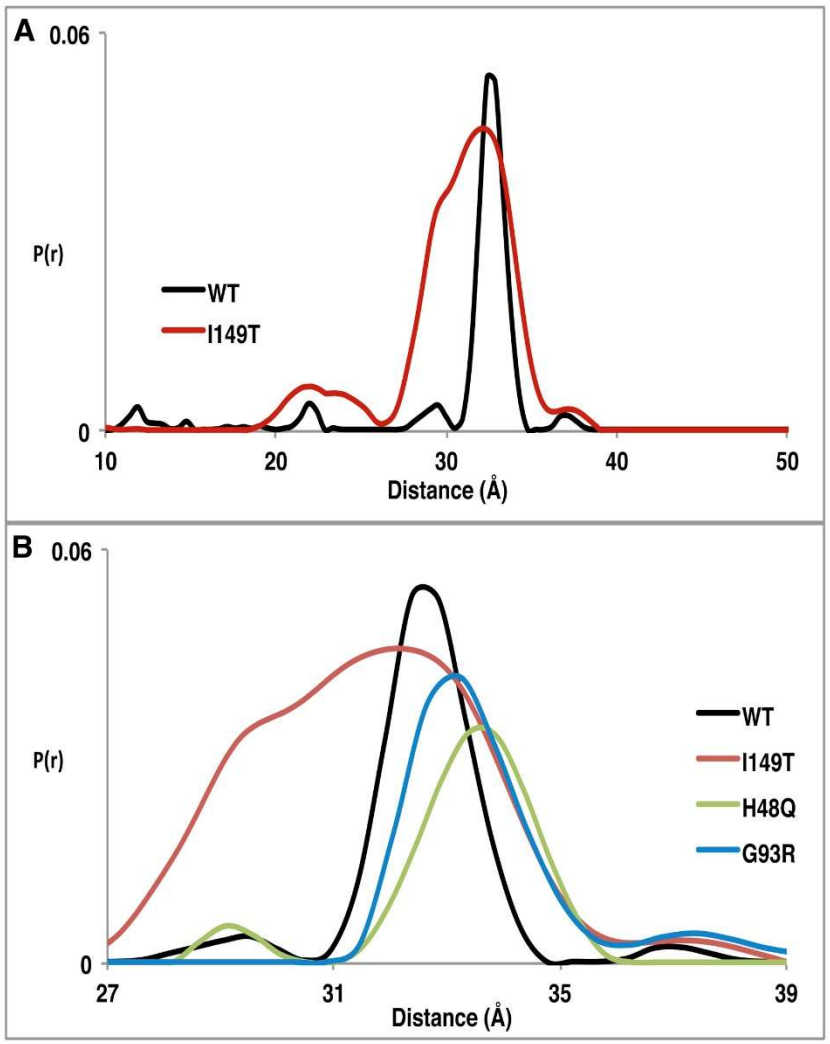

Figure 7. Label-free disease-state detection in SOD1. Cu-Cu DEER distance distributions, P(r) versus distance, are compared for wild-type SOD1 and disease-associated mutants. The measurement exploits the endogenous Cu(II) centers of the homodimer, so no spin label is required, and the shifts between distributions report mutation-induced conformational differences relevant to ALS. *Image adapted with permission from Merz et al. (2014). Copyright 2014 Biophysical Society.*

4.5 Conformational modulation of GPCRs and membrane receptors

G protein-coupled receptors signal by shifting among conformational states, and the population of those states depends on which ligand is bound. Wingler et al. (2019) used DEER to monitor the intracellular

conformational changes of the angiotensin II type 1 receptor and showed that ligands of different functional classes, G protein-biased versus beta-arrestin-biased, stabilize distinct sets of receptor conformations, with biased agonists exerting opposing effects relative to the natural agonist angiotensin II. The resulting conformational maps offer a structural basis for biased signaling, information directly relevant to designing functionally selective drugs.

Morizumi et al. (2019) combined an X-ray structure of Gloeobacter rhodopsin with vibrational and flash-photolysis spectroscopy to characterize its hydrogen-bonding network and photochemistry, and EPR captured the pH-driven oligomerization of the receptor. Together with related work resolving the conformational equilibria of light-activated rhodopsin in nanodiscs (Van Eps et al. 2017), these studies show EPR tracking functional-state changes and quaternary rearrangements in membrane receptors under near-native conditions. Across both examples, EPR converts static receptor structures into the population-level conformational fingerprints that underlie signaling and pharmacology.

4.6 Nucleic acids and CRISPR complexes

Spin labeling is not limited to proteins. Tangprasertchai et al. (2017) applied site-directed spin labeling to double-stranded DNA and used EPR distance measurements to follow the DNA through the steps of CRISPR-Cas9 target recognition, from free DNA, to the Cas9-bound state, to the cleaved product. Each state produced a distinct distance distribution that reports on the degree of DNA unwinding, and combining the EPR distances with molecular dynamics simulations gave atomistic insight into the unwinding and cleavage mechanism (Figure 8). This extends EPR beyond proteins to nucleic acids and nucleoprotein machines, resolving functional states that are difficult to separate by other means.

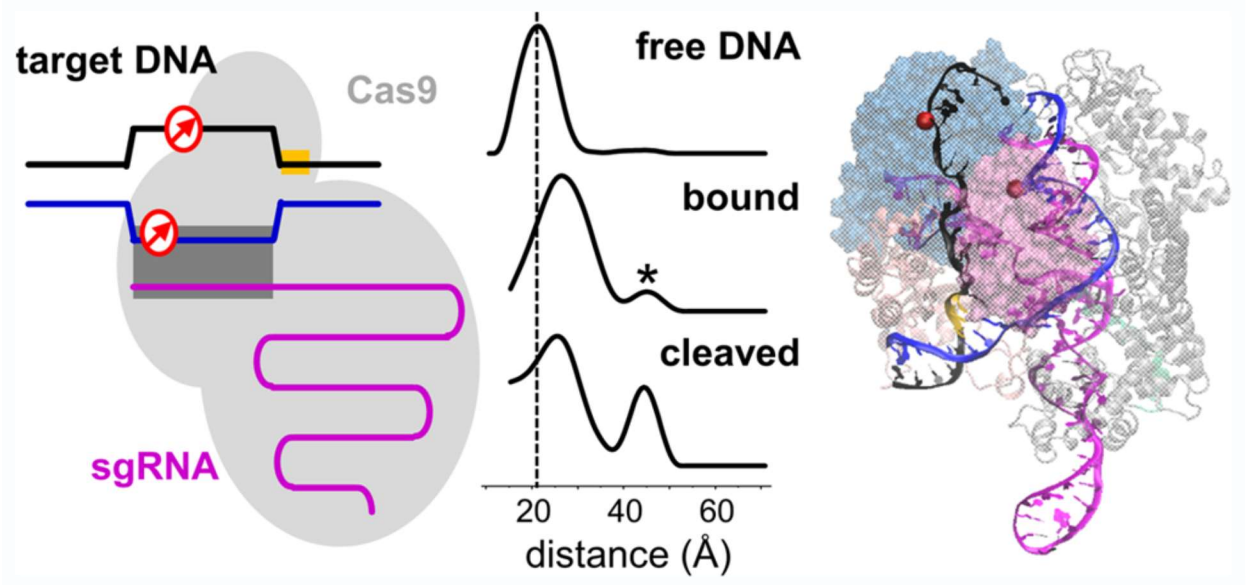

Figure 8. Tracking DNA through CRISPR-Cas9 by EPR. A schematic of spin-labeled target DNA engaging Cas9 and its single guide RNA (left) is paired with the EPR distance distributions for three functional states (right): free DNA, the Cas9-bound state, and the cleaved product. The progressive change in the distributions reports on DNA unwinding during target recognition and cleavage.
Image adapted with permission from Tangprasertchai et al. (2017). Copyright 2017 American Chemical Society.

4.7 Further applications as short case studies

Beyond the systems above, EPR has been applied to a wide range of problems. Three brief examples illustrate the breadth.

Ligand efficacy fingerprinting at the mu-opioid receptor

DEER traced the active, intermediate, and inactive states of the mu-opioid receptor through displacements of transmembrane helices TM4 and TM6, and showed that the population of each state acts as a functional fingerprint of a ligand's efficacy (Zhao et al. 2024). The receptor exposed to a range of drugs, including the super-agonist BU72, and to beta-arrestin1 produced distinct state distributions, linking ligand chemistry to conformational outcome in a way that is directly useful for drug discovery (Figure 9).

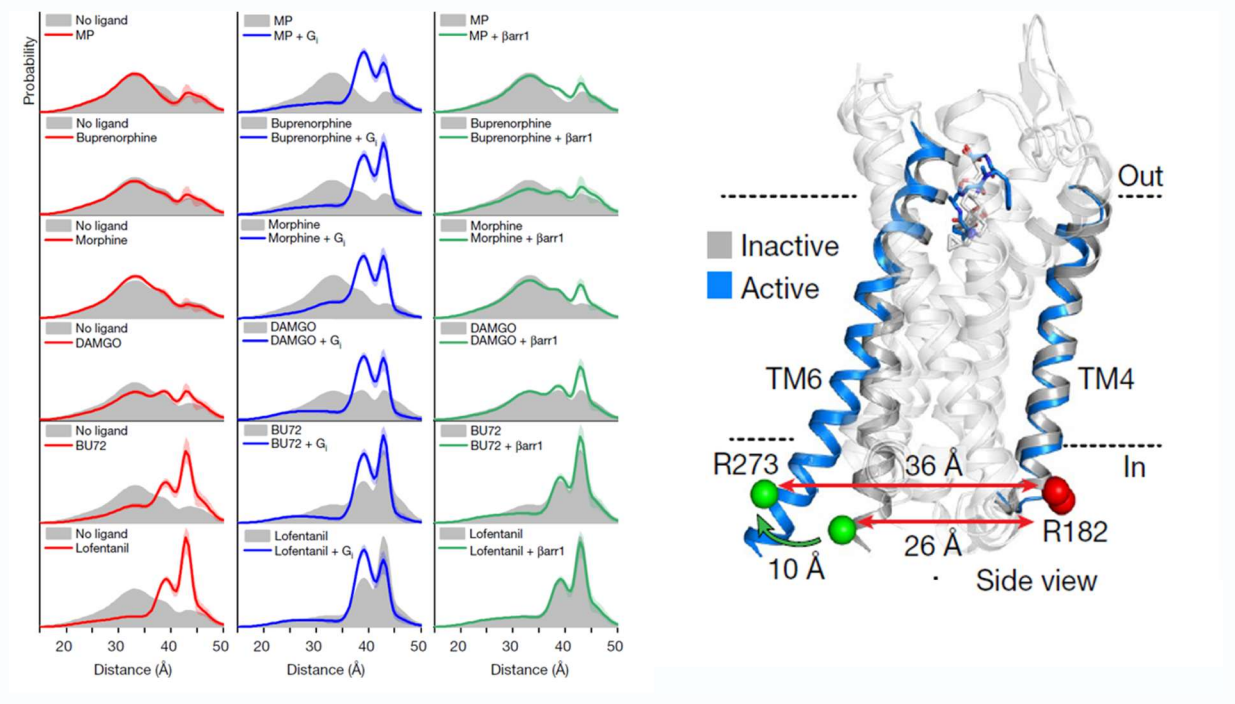

Figure 9. Ligand efficacy as a conformational fingerprint. DEER distance distributions for the mu-opioid receptor under different ligands (left) are read out through the displacement between transmembrane helices TM4 and TM6, which distinguishes inactive and active states (right). The relative populations of the states vary with ligand efficacy, providing a functional fingerprint of each compound. *Adapted from Zhao et al. (2024), licensed under CC BY 4.0.*

In-cell EPR with spin-labeled nanobodies

Gadolinium-labeled nanobodies and sybodies served as conformational reporters in DEER measurements, monitoring epitopes on the outward-facing fraction of an ABC transporter in a membrane, and the approach was extended to show that the transporter MsbA adopts a wide inward-open conformation inside intact E. coli cells (Galazzo et al. 2020, 2022). This demonstrates EPR reaching into the native cellular environment, where most structural methods cannot operate.

Resolving inhibitor binding mechanisms in protein kinases

EPR distance measurements showed that the activation loop of p38-alpha MAP kinase exists as a dynamic ensemble of conformations in solution, and that different classes of inhibitors shift the population toward

distinct structural states, distinguishing conformational selection from induced fit (Roser et al. 2020). This kind of mechanistic read-out is valuable for understanding and optimizing kinase inhibitors.

Further published applications span HIV-1 protease inhibitor resistance (Liu et al. 2016), the conformational heterogeneity of HIV-1 SOSIP envelope trimers relative to crystal and cryo-EM models (Stadtmueller et al. 2018), the apoptosis regulator Bax at the mitochondrial membrane (Bleicken et al. 2014), inhibitor-induced rigidification of bacterial macrophage infectivity potentiator proteins (Perez Carrillo et al. 2025), and quality control of lyophilized protein formulations (Isaev et al. 2025), among others. Several of these are described more fully in the appendix.

5. FATHOM: Making EPR Practical for the Modern Lab

5.1 From specialist technique to standard instrument

The applications in Section 4 share a precondition: access to a pulsed EPR system and the expertise to run it. Historically, this has been the limiting factor. Conventional pulsed EPR has required liquid cryogens, specialized hardware, and an experienced spectroscopist to tune, calibrate, measure, and interpret each measurement. These barriers, rather than any shortcoming in the information EPR provides, are what have kept the technique largely confined to specialist laboratories. The same was once true of high-performance liquid chromatography, mass spectrometry, PCR, and DNA sequencing. Each became a routine laboratory standard only after the instrumentation matured to the point of automation, reliability, and accessibility. FATHOM is designed to bring that same modernization to EPR.

5.2 A superconducting-resonator spectrometer

FATHOM is built around a novel patterned thin-film planar superconducting microstrip resonator, described in detail by Gamble Jarvi et al. (2026). Superconducting resonators offer very high per-spin sensitivity, but they have been difficult to apply to biophysical EPR for two reasons: their small mode volume usually forces sample volumes below one microliter, which sacrifices the concentration sensitivity needed for dilute biological samples, and the large drive currents required to excite the broad lineshapes of spin labels tend to exceed the device's critical current. The FATHOM resonator was engineered specifically to resolve this contradiction, enabling measurement of 3.5 microliter vitrified samples at molecular concentrations below 10 micromolar. The single-spin coupling strength of the device is roughly 0.1 to 0.2 Hz, about an order of magnitude higher than the value near 0.01 Hz typical of conventional three-dimensional EPR resonators. A custom spectrometer with an FPGA-based arbitrary waveform generator and digital intermediate frequency with 500 MHz of instantaneous bandwidth drives the resonator through a 100 W solid-state amplifier, producing 6 ns Gaussian π/2 pulses. The principal system specifications are summarized in Table 2.

Figure 10. The FATHOM automated EPR spectrometer, a benchtop instrument that integrates the superconducting-resonator spectrometer, the cryogen-free cryostat, and the automated sample-handling and analysis software into a single self-contained unit intended for use in a standard laboratory.

Table 2. System specifications of the FATHOM spectrometer, after Gamble Jarvi et al. (2026).

Parameter	Value
Operating frequency	9.5 GHz (X-band)
Operating field	up to 720 mT
Pulse bandwidth	500 MHz
Pulse, delay, and digitizer resolution	1 ns
Shortest π/2 pulse	6 ns (Gaussian)
Conversion efficiency	5 G per √W
HPA power	100 W solid-state
Sample temperature	15 to 89 K
Phase stability	plus or minus 1 degree
Sample volume	3.5 microliters per sample
Cartridge capacity	5 samples

5.3 Sensitivity, stability, and automation

Three advances turn this device into a practical instrument, each corresponding to a requirement that matters in a working laboratory.

Sensitivity

The superconducting resonator delivers the per-spin sensitivity needed to record DEER distance distributions on small volume spin-labeled samples at biologically relevant concentrations, validated in the source work across a range of samples including measurements below 10 micromolar (Gamble Jarvi et al. 2026). In practice, this means less material is consumed, and multiple samples may be placed in a single measurement cartridge for increased measurement throughput.

Stability

The resonator operates in a cryogen-free closed-cycle cryostat held under vacuum, which removes the need for liquid cryogens and stabilizes the resonance frequency for continuous long-term operation on the order of months. The FPGA-based digital intermediate frequency and time-locked digitizer hold phase stability to approximately plus or minus one degree, the consistency required for unattended runs and for comparing measurements across samples and over time.

Automation

Particular attention was paid to software and automation so that a user who is not an EPR specialist can perform unattended, sequential calibration, measurement, and analysis. Samples are loaded as a five-sample cartridge, the operator starts the run and returns when all five are complete, and the results are reported automatically. Beyond convenience, running a uniform automated sequence reduces the systematic bias that can creep into hand-tuned measurements, which is valuable for studies that aim to isolate a single variable, including time-resolved series (Gamble Jarvi et al. 2026).

5.4 Fitting into structural biology and drug-discovery workflows

The combined effect of these advances is that EPR can sit alongside the methods discussed in Sections 3 and 4 as a routine, in-house source of dynamic distance data rather than a specialist outsourcing step. No crystallization is required, the sample volumes and concentrations are compatible with typical biochemical preparations, and the throughput of a multi-sample cartridge suits the iterative screening common in structural biology and drug discovery. In the integrative workflows described earlier, whether refining a flexible Cryo-EM region, generating an AlphaFold ensemble through DEERFold, or mapping a receptor's conformational response to a ligand, FATHOM is intended to make the EPR contribution a practical step within the existing pipeline.

6. Conclusion and Outlook

Structural biology has never been better at determining well-ordered structures, yet the questions that increasingly drive both basic research and drug discovery concern motion, flexibility, and disorder. These are the questions that static, averaged, and predicted structures struggle to answer with high confidence. EPR pulsed dipolar spectroscopy measures precisely this missing information through distance distributions that report directly on conformational ensembles, the breadth of a flexible region, and the populations of coexisting states, over biologically relevant length scales and with no ceiling on molecular size.

The case studies overviewed in this paper show that the value is not hypothetical. EPR has refined and tested Cryo-EM models of transport cycles, turned single AlphaFold predictions into conformational ensembles, characterized intrinsically disordered proteins that evade other methods, distinguished disease-linked states without any label, mapped the biased signaling of receptors, and followed nucleic acids through the steps of a molecular machine. In each case, the information was complementary to the established methods rather than a substitute for them. EPR is best understood as an additional orthogonal source of evidence in an integrative structural biology that speaks directly to dynamics and heterogeneity.

What has limited the wider use of this information is the instrumentation rather than the utility. The superconducting resonator FATHOM EPR system delivers the sensitivity needed for small volume dilute samples, removes the dependence on liquid cryogens, and automates measurement and analysis so that a non-specialist can obtain reliable distance distributions. This is the same kind of transition that turned chromatography, mass spectrometry, PCR, and sequencing from specialist techniques into everyday laboratory tools.

With routine user-friendly EPR now available, several directions are natural. Distance restraints can be built more deeply into Cryo-EM refinement, AlphaFold ensemble generation, molecular dynamics, and hybrid modeling. In-cell measurements can extend structural questions into the native cellular environment. In drug discovery, conformational fingerprinting of receptors and the direct study of intrinsically disordered targets open approaches that static structures cannot support. The unifying theme is that measuring how molecules move, and how many shapes they adopt, is becoming a standard part of describing what they are. FATHOM makes that measurement routine.

Appendix

This appendix collects additional published applications of EPR and pulsed dipolar spectroscopy, presented as short case studies. They extend the themes of Section 4 into immunology, apoptosis, antimicrobial and genome-editing targets, muscle biology, biopharmaceutical formulation, and materials science.

A.1 HIV-1 protease: conformational sampling and inhibitor resistance

HIV-1 protease is a small homodimeric enzyme and a major antiretroviral target whose flap regions open and close over the active site. Liu et al. (2016) used DEER to characterize the conformational landscape of the protease, resolving the ensemble of flap states from closed through semi-open to wide-open, and showing how clinically relevant mutations and bound inhibitors shift the populations among them. Because drug resistance often manifests as a change in conformational sampling rather than in any single static structure, the distance distributions give a direct, quantitative readout of how a mutation or an inhibitor remodels the flap equilibrium, well matched to the iterative testing of inhibitor candidates.

A.2 HIV-1 envelope trimer conformations for immunogen design

The HIV-1 envelope glycoprotein (Env) trimer is the sole target of neutralizing antibodies and is highly dynamic, which complicates vaccine design. Stadtmueller et al. (2018) applied DEER to soluble SOSIP Env trimers and to their complexes with antibodies and with the CD4 receptor, mapping multiple coexisting conformations and showing that the soluble immunogen samples states with similarities to Env on native virions. By revealing which conformations a given antibody or ligand stabilizes, the measurements connect the dynamic behavior of the immunogen to its antigenic surface, information that static structures of individual states cannot supply on their own.

A.3 The apoptosis regulator Bax: resting monomer and active membrane oligomer

Bax converts from an inactive cytosolic monomer to membrane-inserted oligomers that permeabilize the mitochondrial outer membrane during apoptosis. Two EPR studies capture complementary parts of this transition. Barnes et al. (2017) combined NMR with DEER and found the conformational distribution of monomeric Bax to be homogeneous, a single well-defined state rather than a pre-existing mixture poised for activation. Bleicken et al. (2014) then used DEER to build a structural model of the active, membrane-embedded form, and here modulation depth analysis was central: comparing the modulation depth of spin-diluted and undiluted samples separated the inter-monomer distances within the oligomer from intramolecular distances, establishing the dimeric building block of active Bax at the membrane. The pair shows EPR resolving both the resting state and the assembled machine, and illustrates modulation depth as a direct reporter of oligomeric state.

A.4 Antimicrobial targets: macrophage infectivity potentiator proteins

Macrophage infectivity potentiator (MIP) proteins are virulence factors in pathogenic bacteria and protozoans and are emerging antimicrobial targets. Perez Carrillo et al. (2025) combined crystallography, EPR, and other biophysical methods to study MIP proteins bound to fluorinated pipecolic acid inhibitors, using spin-label distance measurements to characterize the protein's conformational dynamics and how

inhibitor binding rigidifies it. The study shows EPR contributing the dynamic dimension of a structure-based drug-discovery campaign, distinguishing how candidate inhibitors restrain a flexible target rather than only where they bind.

A.5 CRISPR-Cas12a target discrimination

Building on the Cas9 study in Section 4.6, Singh et al. (2023) applied site-directed spin labeling and EPR to CRISPR-Cas12a and showed that a DNA unwinding equilibrium acts as a checkpoint for target discrimination. By measuring distance distributions that report on the extent of R-loop formation and DNA unwinding for matched and mismatched targets, they linked the position of this conformational equilibrium to the enzyme's ability to reject off-target sequences. The result ties a measurable conformational state to fidelity, a property of direct interest for improving the specificity of genome-editing tools.

A.6 Mapping a protein interaction interface with Rosetta and DEER

ExoU, a type III secretion phospholipase toxin, is activated by ubiquitin, but its binding interface was unknown. Tessmer et al. (2018) combined DEER distance restraints with Rosetta computational docking to identify the ubiquitin-binding interface on ExoU, using a sparse set of experimental distances to disambiguate among many candidate models. This is a clear case of EPR acting as a restraint provider in integrative modeling, the same role described in Sections 3 and 4 for Cryo-EM and AlphaFold, applied here to a protein-protein interaction.

A.7 Muscle proteins, oxidative stress, and protein turnover

EPR has a long record in muscle biophysics and protein turnover. Moen et al. (2014) reviewed how site-directed spin labeling resolves the effects of oxidative stress on muscle proteins such as myosin, relating oxidative modification to changes in structural dynamics and function. Stevens et al. (2019) used EPR distance measurements to explore the TRIM fold of MuRF1, a muscle-specific E3 ubiquitin ligase that tags proteins for degradation, revealing a canonical antiparallel coiled-coil architecture and an extended COS-box. Together these studies show EPR reporting on both the damage that marks proteins for turnover and the structure of the machinery that carries it out.

A.8 Antigen processing by the TAP transporter

The transporter associated with antigen processing (TAP) loads antigenic peptides into the endoplasmic reticulum for presentation to the immune system. Herget et al. (2011) attached spin labels to antigenic peptides and used EPR to determine the conformation of the peptide while bound to TAP, showing that the bound peptide adopts a defined, bent conformation with its central residues bulged out. This is an example of EPR reading out the conformation of a small ligand within a large membrane-protein complex, a measurement that is difficult for methods requiring the whole assembly to be well ordered.

A.9 Biopharmaceutical formulation and quality control

EPR also serves biopharmaceutical development and quality control. Isaev et al. (2025) used pulsed EPR to probe the folding and local molecular environment of proteins in the lyophilized solid state, where conventional structural methods are hard to apply, providing a way to assess whether a freeze-dried protein drug retains its native fold. Sanaeifar et al. (2022) used spin-probe EPR to follow the macro- and nanoscale

effects of ethanol on bovine serum albumin gelation and the release of the drug naproxen, characterizing formulation microstructure relevant to drug delivery. Juarez-Calderon et al. (2009) exploited the stable radicals generated in acetylsalicylic acid by ionizing radiation to evaluate EPR dosimetry of pharmaceutical preparations, relevant to radiation sterilization. These examples extend EPR from structural biology into formulation science and manufacturing.

A.10 Spin-active nanomaterials: functional metallofullerenes

Finally, EPR-active materials are themselves an application area. Wang and Wang (2019) reviewed functional endohedral metallofullerenes, carbon cages encapsulating metal atoms or clusters, whose paramagnetic centers underpin uses in nanomedicine, including gadolinium metallofullerenes as MRI contrast and antitumor agents, as well as in magnetics and electronics. These spin-bearing nanomaterials connect the magnetic-resonance principles used throughout this paper to a broader landscape of designed paramagnetic systems.

References

Barnes, C. A., Mishra, P., Baber, J. L., Strub, M. P., & Tjandra, N. (2017). Conformational heterogeneity in the activation mechanism of Bax. Structure, 25(8), 1310-1316. https://doi.org/10.1016/j.str.2017.06.009

Bleicken, S., Jeschke, G., Stegmueller, C., Salvador-Gallego, R., Garcia-Saez, A. J., & Bordignon, E. (2014). Structural model of active Bax at the membrane. Molecular Cell, 56(4), 496-505. https://doi.org/10.1016/j.molcel.2014.09.022

Clore, G. M., & Iwahara, J. (2009). Theory, practice, and applications of paramagnetic relaxation enhancement for the characterization of transient low-population states of biological macromolecules and their complexes. Chemical Reviews, 109(9), 4108-4139. https://doi.org/10.1021/cr900033p

del Alamo, D., DeSousa, L., Nair, R. M., Rahman, S., Meiler, J., & Mchaourab, H. S. (2022). Integrated AlphaFold2 and DEER investigation of the conformational dynamics of a pH-dependent APC antiporter. Proceedings of the National Academy of Sciences, 119(34), e2206129119. https://doi.org/10.1073/pnas.2206129119

Frank, J., & Ourmazd, A. (2016). Continuous changes in structure mapped by manifold embedding of single-particle data in cryo-EM. Methods, 100, 61-67. https://doi.org/10.1016/j.ymeth.2016.02.007

Galazzo, L., Meier, G., Timachi, M. H., Hutter, C. A. J., Seeger, M. A., & Bordignon, E. (2020). Spin-labeled nanobodies as protein conformational reporters for electron paramagnetic resonance in cellular membranes. Proceedings of the National Academy of Sciences, 117(5), 2441-2448. https://doi.org/10.1073/pnas.1913737117

Galazzo, L., Meier, G., Januliene, D., Parey, K., De Vecchis, D., Striednig, B., Hilbi, H., Schaefer, L. V., Kuprov, I., Moeller, S., Bordignon, E., & Seeger, M. A. (2022). The ABC transporter MsbA adopts the wide inward-open conformation in E. coli cells. Science Advances, 8(41), eabn6845. https://doi.org/10.1126/sciadv.abn6845

Galazzo, L., Teucher, M., & Bordignon, E. (2022). Orthogonal spin labeling and pulsed dipolar spectroscopy for protein studies. In Methods in Enzymology. Academic Press.

Gamble Jarvi, A. R., Mohebbi, H. R., Raval, I., Culzac, O., Erickson, J., Hegazy, S., Carkner, D., Wiles, A., Cory, D. G., & Borneman, T. W. (2026). Biophysical EPR using superconducting resonators. https://doi.org/10.48550/arXiv.2606.23952.

Herget, M., Baldauf, C., Scholz, C., Parcej, D., Wiesmuller, K. H., Tampe, R., Abele, R., & Bordignon, E. (2011). Conformation of peptides bound to the transporter associated with antigen processing (TAP). Proceedings of the National Academy of Sciences, 108(4), 1349-1354. https://doi.org/10.1073/pnas.1012355108

Honegger, P., Di Pietro, M. E., Castiglione, F., Vaccarini, C., Quant, A., Steinhauser, O., Schröder, C., & Mele, A. (2021). The intermolecular NOE depends on isotope selection: short range vs long range behavior. The Journal of Physical Chemistry Letters, 12, 8658-8663. https://doi.org/10.1021/acs.jpclett.1c02253

Isaev, N., Lo Presti, K., & Friess, W. (2025). Insights into folding and molecular environment of lyophilized proteins using pulsed electron paramagnetic resonance spectroscopy. Molecular Pharmaceutics, 22(1), 424-432. https://doi.org/10.1021/acs.molpharmaceut.4c01008

Juarez-Calderon, J. M., Negron-Mendoza, A., Gomez-Vidales, V., & Ramos-Bernal, S. (2009). Study of dosimetric properties of acetylsalicylic acid in pharmaceutical preparations by EPR spectroscopy. Journal of Radioanalytical and Nuclear Chemistry, 280(2), 245-249. https://doi.org/10.1007/s10967-009-0506-8

Konermann, L., Pan, J., & Liu, Y.-H. (2011). Hydrogen exchange mass spectrometry for studying protein structure and dynamics. Chemical Society Reviews, 40, 1224-1234. https://doi.org/10.1039/c0cs00113a

Lazar, T., Connor, A., DeLisle, C. F., Burger, V., & Tompa, P. (2025). Targeting protein disorder: the next hurdle in drug discovery. Nature Reviews Drug Discovery. https://doi.org/10.1038/s41573-025-01220-6

Liu, Z., Casey, T. M., Blackburn, M. E., Huang, X., Pham, L., de Vera, I. M. S., Carter, J. D., Kear-Scott, J. L., Veloro, A. M., Galiano, L., & Fanucci, G. E. (2016). Pulsed EPR characterization of HIV-1 protease conformational sampling

and inhibitor-induced population shifts. Physical Chemistry Chemical Physics, 18(8), 5819-5831. https://doi.org/10.1039/c5cp04556h

Matsumura, M., Wozniak, J. A., Sun, D. P., & Matthews, B. W. (1989). Structural studies of mutants of T4 lysozyme that alter hydrophobic stabilization. Journal of Biological Chemistry, 264(28), 16059-16066. https://doi.org/10.2210/pdb3LZM/pdb

Merz, G. E., Borbat, P. P., Pratt, A. J., Getzoff, E. D., Freed, J. H., & Crane, B. R. (2014). Copper-based pulsed dipolar ESR spectroscopy as a probe of protein conformation linked to disease states. Biophysical Journal, 107(7), 1669-1674. https://doi.org/10.1016/j.bpj.2014.07.068

Moen, R. J., Klein, J. C., & Thomas, D. D. (2014). Electron paramagnetic resonance resolves effects of oxidative stress on muscle proteins. Exercise and Sport Sciences Reviews, 42(1), 30-36. https://doi.org/10.1249/JES.0000000000000004

Morizumi, T., Ou, W.-L., Van Eps, N., Inoue, K., Kandori, H., Brown, L. S., & Ernst, O. P. (2019). X-ray crystallographic structure and oligomerization of Gloeobacter rhodopsin. Scientific Reports, 9, 11283. https://doi.org/10.1038/s41598-019-47445-5

Narunsky, A., Ashkenazy, H., Kolodny, R., & Ben-Tal, N. (2015). Using ConTemplate and the PDB to explore conformational space: on the detection of rare protein conformations. BMC Bioinformatics, 16(Suppl 3), A3. https://doi.org/10.1186/1471-2105-16-S3-A3

Perez Carrillo, V. H., Whittaker, J. J., Wiedemann, C., Harder, J.-M., Lohr, T., Jamithireddy, A. K., Dajka, M., Goretzki, B., Joseph, B., Guskov, A., Harmer, N. J., Holzgrabe, U., & Hellmich, U. A. (2025). Structure and dynamics of macrophage infectivity potentiator proteins from pathogenic bacteria and protozoans bound to fluorinated pipecolic acid inhibitors. Journal of Medicinal Chemistry, 68(5), 5926-5941. https://doi.org/10.1021/acs.jmedchem.5c00134

Roser, P., Weisner, J., Stehle, J., Rauh, D., & Drescher, M. (2020). Conformational selection vs. induced fit: insights into the binding mechanisms of p38-alpha MAP kinase inhibitors. Chemical Communications, 56(62), 8818-8821. https://doi.org/10.1039/d0cc02539a

Roy, A. S., Tsay, K., Borbat, P. P., Destefano, A., Han, S., Srivastava, M., & Freed, J. H. (2025). Detection of mutation-induced conformational changes in an intrinsically disordered protein by double quantum coherence electron spin resonance methodology. Journal of the American Chemical Society. https://doi.org/10.1021/jacs.5c16298

Sanaeifar, N., Mader, K., & Hinderberger, D. (2022). Macro- and nanoscale effect of ethanol on bovine serum albumin gelation and naproxen release. International Journal of Molecular Sciences, 23(13), 7352. https://doi.org/10.3390/ijms23137352

Singh, J., Liu, K. G., Allen, A., Jiang, W., & Qin, P. Z. (2023). A DNA unwinding equilibrium serves as a checkpoint for CRISPR-Cas12a target discrimination. Nucleic Acids Research, 51(16), 8730-8743. https://doi.org/10.1093/nar/gkad636

Stadtmueller, B. M., Bridges, M. D., Dam, K. M., Lerch, M. T., Huey-Tubman, K. E., Hubbell, W. L., & Bjorkman, P. J. (2018). DEER spectroscopy measurements reveal multiple conformations of HIV-1 SOSIP envelopes that show similarities with envelopes on native virions. Immunity, 49(2), 235-246. https://doi.org/10.1016/j.immuni.2018.06.017

Stevens, M., Franke, B., Skorupka, K. A., Cafiso, D. S., Pornillos, O., Mayans, O., & Norman, D. G. (2019). Exploration of the TRIM fold of MuRF1 using EPR reveals a canonical antiparallel structure and extended COS-box. Journal of Molecular Biology, 431(15), 2900-2909. https://doi.org/10.1016/j.jmb.2019.05.025

Stock, C., Hielkema, L., Tascon, I., Wunnicke, D., Oostergetel, G. T., Azkargorta, M., Paulino, C., & Haenelt, I. (2018). Cryo-EM structures of KdpFABC suggest a K+ transport mechanism via two inter-subunit half-channels. Nature Communications, 9, 4971. https://doi.org/10.1038/s41467-018-07319-2

Tangprasertchai, N. S., Di Felice, R., Zhang, X., Slaymaker, I. M., Vazquez Reyes, C., Jiang, W., Rohs, R., & Qin, P. Z. (2017). CRISPR-Cas9 mediated DNA unwinding detected using site-directed spin labeling. ACS Chemical Biology, 12(6), 1489-1493. https://doi.org/10.1021/acschembio.6b01137

Tessmer, M. H., Anderson, D. M., Pickrum, A. M., Riegert, M. O., Moretti, R., Meiler, J., Feix, J. B., & Frank, D. W. (2018). Identification of a ubiquitin-binding interface using Rosetta and DEER. Proceedings of the National Academy of Sciences, 115(3), 525-530. https://doi.org/10.1073/pnas.1716861115

Van Eps, N., Caro, L. N., Morizumi, T., Kusnetzow, A. K., Szczepek, M., Hofmann, K. P., Bayburt, T. H., Sligar, S. G., Ernst, O. P., & Hubbell, W. L. (2017). Conformational equilibria of light-activated rhodopsin in nanodiscs. Proceedings of the National Academy of Sciences, 114(16), E3268-E3275. https://doi.org/10.1073/pnas.1620405114

Wang, T., & Wang, C. (2019). Functional metallofullerene materials and their applications in nanomedicine, magnetics, and electronics. Small, 15(48), 1901522. https://doi.org/10.1002/smll.201901522

Wingler, L. M., Elgeti, M., Hilger, D., Latorraca, N. R., Lerch, M. T., Staus, D. P., Dror, R. O., Kobilka, B. K., Hubbell, W. L., & Lefkowitz, R. J. (2019). Angiotensin analogs with divergent bias stabilize distinct receptor conformations. Cell, 176(3), 468-478. https://doi.org/10.1016/j.cell.2018.12.005

Woldeyes, R. A., Sivak, D. A., & Fraser, J. S. (2014). E pluribus unum, no more: from one crystal, many conformations. Current Opinion in Structural Biology, 28, 56-62. https://doi.org/10.1016/j.sbi.2014.07.005

Wu, T., Stein, R. A., Kao, T.-Y., Brown, B., & Mchaourab, H. S. (2025). Modeling protein conformational ensembles by guiding AlphaFold2 with double electron-electron resonance (DEER) distance distributions. Nature Communications. https://doi.org/10.1038/s41467-025-62582-4

Zhang, R., Jagessar, K. L., Brown, M., Polasa, A., Stein, R. A., Moradi, M., Karakas, E., & Mchaourab, H. S. (2024). Conformational cycle of a protease-containing ABC transporter in lipid nanodiscs reveals the mechanism of cargo-protein coupling. Nature Communications, 15. https://doi.org/10.1038/s41467-024-53420-0

Zhao, J., Elgeti, M., O'Brien, E. S., Sar, C. P., Ei Daibani, A., Heng, J., Sun, X., Che, T., & Chen, C. (2024). Ligand efficacy modulates conformational dynamics of the mu-opioid receptor. Nature, 629(8011), 474-480. https://doi.org/10.1038/s41586-024-07295-2